Published in Journal of Crystal Growth 251, issues 1-4, 697-700, 2003
which should be used for any reference to this work

Continuous wave operation of quantum cascade lasers

M. Beck[a,*], D. Hofstetter[a], T. Aellen[a], S. Blaser[a], J. Faist[a], U. Oesterle[b], E. Gini[c]

[a] *Institute of Physics, University of Neuchâtel, Rue Breguet 1, CH-2000 Neuchâtel, Switzerland*
[b] *Institute of Micro- and Optoelectronics, ETH Lausanne, Switzerland*
[c] *Center for Micro- and Nanosciences, ETH Zurich, Switzerland*

Abstract

Continuous wave (CW) operation of quantum cascade lasers is reported up to temperatures of 312 K. The devices were fabricated as buried heterostructure lasers and episide-down mounted for improved heat dissipation. Fabry–Perot lasers emitted 17 mW of continuous optical power at 292 K and still 3 mW at 311 K at $\lambda = 9.12\,\mu m$. Distributed feedback quantum cascade lasers showed CW single-mode operation up to 260 K at $\lambda = 9.0\,\mu m$ with a side mode suppression rate better than 30 dB.

PACS: 42.55.Px; 42.60.Pk; 78.45.+h; 78.67.−w

Keywords: A1. Intersubband; A3. Molecular beam epitaxy; B3. Quantum cascade laser

1. Introduction

Mid-infrared lasers have traditionally an important field of applications in the sensor area like industrial process monitoring, medical diagnostics, and environmental sensing since most gas molecules have their vibrational modes in this wavelength range. A new class of semiconductor lasers—quantum cascade (QC) lasers [1]—has become a promising alternative to conventional diode lasers in the mid-infrared with pulsed operation above room temperature between 3.4 to 16 μm [2,3]. However, continuous wave (CW) operation of QC lasers has remained limited to cryogenic temperatures below 210 K [4] imposing a strong technological limitation for all applications that require narrow linewidths and/or high-frequency modulation. The maximum CW operating temperature increased only for 60 K (from 145 to 210 K between 1995 and 2001). Different methods like junction down mounting or dielectric-metal-based back facet coatings [5] had been tried to push the CW operating temperature towards higher values. However, all attempts failed quite systematically due to very high threshold current densities which led to overheating of the device. For this reason, it was essential to (i) minimize the threshold current density and (ii) use a laser geometry that maximizes heat dissipation from the active region and minimizes thermal stress within the active region.

*Corresponding author. Tel.: +41-32-718-2947,
Fax: +41-32-718-2901.
E-mail address: mattias.beck@unine.ch (M. Beck).

2. Fabrication

We present buried heterostructure QC lasers with a four-quantum well (QW) active region

based on a double phonon resonance [6] with an improved waveguiding scheme and better heat dissipation for high temperature CW operation. The laser structure is grown by molecular beam epitaxy (MBE) using ternary InGaAs and InAlAs alloys lattice matched to an n-doped InP substrate. The QC laser active material consists of 35 periods, each comprising a partially n-doped injector region and the undoped four QW active region, embedded in an optical waveguide formed on one side by the InP substrate and a 0.2 μm thick InGaAs layer and on the other side by an upper InGaAs layer and an InP top cladding layer. The structure of the active region is described in detail in Ref. [7]. The four QW design makes use of short lifetime of the lower lasing state and the good injection efficiency into the upper lasing state. The presence of three coupled lower energy states in the active region allowing the emission of two optical phonons from the lower laser level increases the ratio between the upper and lower state population (as compared to single-phonon three QW active region), decreases the threshold current density, and increases the slope efficiency and maximum power. Additionally, growth conditions and the doping concentration of the active region were optimized to further reduce the threshold current density. As a consequence, the threshold current density at 300 K dropped to a value as low as 3 kA/cm^2.

Buried heterostructure lasers were fabricated by chemical wet etching of 5 μm deep and 9–15 μm wide ridge waveguides using an SiO_2 mask followed by regrowth of 5 μm of non-intentionally doped InP by metal-organic chemical vapor phase epitaxy (MOVPE) to form the planarized buried heterostructure [8]. The SiO_2 layer on top of the laser ridge was removed after regrowth and ohmic contacts were evaporated on top of the highly doped cladding layer. Substrate thinning and standard back metalization completed the laser fabrication. Devices were then cleaved into 0.75 mm long lasers, soldered junction down onto a diamond platelet and finally facet coated by a ZnSe/PbTe high-reflectivity ($R = 0.7$) layer pair. The choice of a buried stripe greatly improves the heat transport by allowing heat flow from all sides of the active region due to the much higher thermal conductivity of InP compared to ternary III–V compounds and insulating SiN layers used in the conventional ridge geometry of QC lasers. Moreover, the small refractive index difference between the waveguide core and lateral InP allowed to make very narrow waveguides without having excessive losses. Additionally, the narrow stripe geometry also decreases the total amount of strain that builds up in a material subjected to a very strong temperature gradient [7].

3. Results

The optical power emitted under continuous wave operation was measured using a calibrated thermopile detector which was mounted directly in front of the laser facet. At room temperature (292 K), 15 μm wide FP-lasers emitted up to 17 mW of optical power per facet at a drive current of 600 mA (Fig. 1) resulting in a slope efficiency $\eta = dP/dI$ of 99 mW/A and a wall plug efficiency of 0.33% per facet. This device could be operated up to 311 K with a maximum optical power of 3 mW ($\eta = 52$ mW/A). The threshold current I_{th} increased from 415 mA at 292 K (corresponding to a threshold current density J_{th} of 3.7 kA/cm^2) to 540 mA at 311 K ($J_{th} = 4.8$ kA/cm^2). The threshold voltage V_{th} increased from 7.5 to 8.1 V over the measured temperature range.

FP lasers with the same cavity length but a slightly narrower stripe width of 12 μm exhibited a

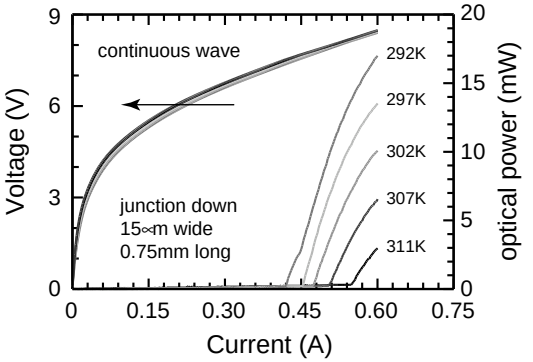

Fig. 1. Voltage bias and CW optical power from a single laser facet of an FP laser as a function of drive current for various heat sink temperatures. The laser is 0.75 mm long and 15 μm wide.

threshold current of 390 mA ($J_{th} = 4.3\,kA/cm^2$ at a voltage bias $U = 7.6\,V$) and a slope efficiency $\eta = 101\,mW/A$ at 292 K. This device emitted 13 mW of optical power from a single facet at a driving current of 550 mA resulting in a wall plug efficiency of 0.275% per facet. For these devices, continuous wave operation was observed up to 312 K. At this temperature, the threshold current increased to 520 mA ($J_{th} = 5.8\,kA/cm^2$), while still more than 1 mW of output power was emitted at 550 mA.

The CW spectral properties were analyzed with a Fourier transform infrared spectrometer ($0.125\,cm^{-1}$ resolution). When changing the injection current from 395 to 530 mA, we observed single-mode operation with a linear tuning as function of the injected power (Fig. 2a). At a constant temperature of 292 K, we measured frequency tuning from $1096.74\,cm^{-1}$ (395 mA) to $1094.54\,cm^{-1}$ (530 mA) resulting in a linear tuning coefficient of $\Delta\upsilon/\Delta P = -1.51\,cm^{-1}/W$. At constant current of 530 mA, the emission frequency of the laser shifts from $1094.54\,cm^{-1}$ at 292 K to $1092.90\,cm^{-1}$ at 313 K resulting in a tuning coefficient of $\Delta\upsilon/\Delta T = -0.078\,cm^{-1}/K$ (Fig. 2b). Keeping in mind that the above temperature tuning is based on the averaged refractive index change across the entire laser structure, we can calculate a preliminary value for the thermal resistance using the formula $R_{th} = \Delta T/\Delta P = (\Delta\upsilon/\Delta P) \times (\Delta\upsilon/\Delta T)^{-1}$. With the above tuning rates, we find $R_{th} = 19.4\,K/W$, or, using the device area of $750\,\mu m \times 12\,\mu m$, a thermal conductance G_{th} of $574\,W/K\,cm^2$. Single-mode emission was observed for this device over the whole investigated current and temperature range with a side mode suppression ratio better than 30 dB.

Far-field distributions in the two directions parallel and perpendicular to the grown layers were measured on the 15 μm wide devices under pulsed conditions and at four representative injection currents. In both directions, we observed Gaussian distributions which did not change at higher injection. In the direction parallel to the layers, we found a far-field angle of 40° full-width at half-maximum (FWHM). In the other direction, the angle was on the order of 80°. The Gaussian distributions prove that the device oscillates in its fundamental lateral and transverse mode, which makes this laser much more convenient for potential applications.

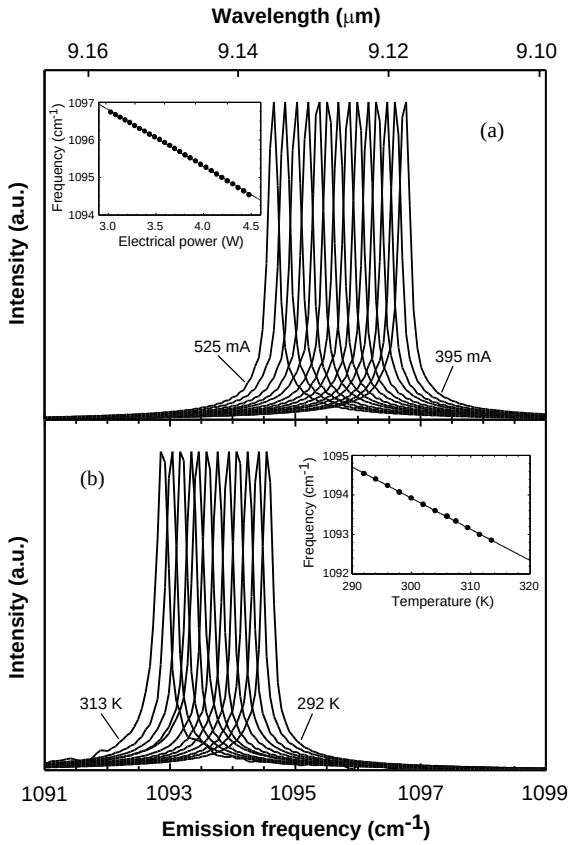

Fig. 2. (a) CW spectra as a function of injection current. The emission spectra were measured at a constant temperature of 292 K for injection currents ranging from 395 to 525 mA in steps of 10 mA. Inset: emitted peak frequency in dependence of the electrical input power at constant temperature. (b) Series of CW emission spectra as a function of temperature at a constant drive current of 530 mA. The temperature varies from 292 to 313 K. Inset: measured temperature dependence of the center emission frequency for $I = 530\,mA$.

Buried heterostructure distributed feedback (DFB) lasers were fabricated from the same active region material. The grating with a 1.435 μm period for an emission frequency at $1106\,cm^{-1}$ was holographically defined using a 488 nm Ar-ion laser, then etched by wet chemical etching to a depth of 180 nm into the upper 200 nm thick InGaAs waveguide layer, and then overgrown by InP (top cladding layer). The buried heterostruc-

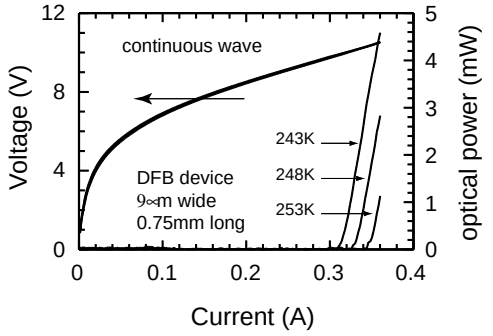

Fig. 3. Bias voltage and optical power from a single laser facet of a HR-coated DFB laser as a function of drive current for various heat sink temperatures.

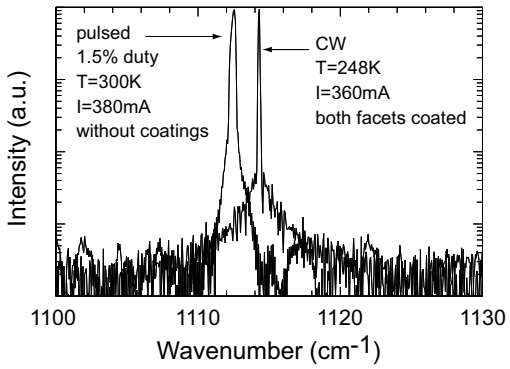

Fig. 4. Emission spectra of a DFB device before and after facet coating. The left peak at 1112.8 cm^{-1} belongs to the spectrum of the uncoated laser measured in pulsed mode at room temperature.

ture was fabricated with a narrower active region width (9 μm for the DFB-devices, compared to 12 or 15 μm of the FP lasers) to reduce the current consumption. DFB lasers could be operated in continuous mode up to 260 K on a thermoelectric cooler (Fig. 3). At 243 K, lasing action was observed above a threshold current of 310 mA ($J_{th} = 4.6\,kA/cm^2$) with a maximum measured optical power of 4.6 mW at 360 mA ($\eta = 92\,mW/A$). At 253 K, 1 mW of optical power was measured per facet.

Fig. 4 shows the lasing spectra of the uncoated DFB device in pulsed mode and of the same device with HR-coatings driven in continuous wave. The spectra for the uncoated laser were measured at a duty cycle of 1.5% for various injection currents at $T = 300\,K$ and showed single-mode emission over the whole current range. The emission peak at 1112.8 cm^{-1}, measured at $I = 380\,mA$, has a linewidth of 0.25 cm^{-1}. The same laser but with HR coatings and operated in CW shows single-mode emission with a narrow peak around 1114.3 cm^{-1} at the maximum operating current and $T = 248\,K$. In CW mode, we observed single-mode emission over the whole temperature and current range (243–253 K, 310–360 mA) with a narrow linewidth (below the resolution limit of our FTIR of 0.125 cm^{-1}) and a high side mode suppression ratio (> 30 dB).

Acknowledgements

The authors gratefully acknowledge M. Ebnöther for technical assistance with the lateral InP regrowth. This work was financially supported by the Swiss National Science Foundation and the Science Foundation of the European Community under IST project SUPERSMILE.

References

[1] J. Faist, F. Capasso, D.L. Sivco, C. Sirtori, A.L. Hutchinson, A.Y. Cho, Science 264 (1994) 553.
[2] J. Faist, F. Capasso, D.L. Sivco, A.L. Hutchinson, S.-N.G. Chu, A.Y. Cho, Appl. Phys. Lett. 72 (1998) 680.
[3] M. Rochat, D. Hofstetter, M. Beck, J. Faist, Appl. Phys. Lett. 79 (2001) 4271.
[4] B. Ishaug, W.-Y. Hwang, J. Um, B. Guo, H. Lee, C.-H. Lin, Appl. Phys. Lett. 79 (2001) 1745.
[5] C. Gmachl, A.M. Sergent, A. Tredicucci, F. Capasso, A.L. Hutchinson, D.L. Sivco, J.N. Baillargeon, S.-N.G. Chu, A.Y. Cho, IEEE Photon. Technol. Lett. 11 (1999) 1369.
[6] D. Hofstetter, M. Beck, T. Aellen, J. Faist, U. Oesterle, M. Ilegems, E. Gini, H. Melchior, Appl. Phys. Lett. 78 (2001) 1964.
[7] M. Beck, D. Hofstetter, T. Aellen, J. Faist, U. Oesterle, M. Ilegems, E. Gini, H. Melchior, Science 295 (2002) 301.
[8] M. Beck, J. Faist, U. Oesterle, M. Ilegems, E. Gini, H. Melchior, IEEE Photon. Technol. Lett. 12 (2000) 1450.